[1] Yuan Chai
[2] Feng Qiu
[3] Xiaoling Li

Design of High-Precision Motion Planning and Optimization Strategies Based on Redundant Robot Arms

Journal of Electrical Systems

Abstract: - Robot arms play a pivotal role as actuators in industrial production, finding widespread applications across diverse sectors. Redundant robot arms, distinguished by their surplus joint degrees of freedom relative to task requirements, offer a spectrum of advanced performance capabilities. Within the realm of redundant robot arms, motion planning emerges as a cornerstone area of investigation. This paper presents an innovative approach to high-precision motion planning within the field of redundant robot arms. First, the pseudo-inverse scheme prevalent in robot arm motion planning is noted. Subsequently, using a process of discretizing the difference formula, we finally propose a high-precision motion planning scheme. Finally, the effectiveness and superiority of this novel motion planning method are strictly evaluated through the combination of theoretical analysis and simulation experiments. Notably, these experiments utilized a comprehensive range of scenarios, including a five-link manipulator operated in a flat environment and the well-known UR 5 robot arm. This extended discussion highlights the profound significance of motion planning in the context of redundant robot arms, demonstrating innovative advances in improving the precision and effectiveness of robot arm operations. Through careful analysis and experiments, this paper makes substantial contributions to the development of robot arm research, which is expected to improve performance and universal functionality in industrial applications.

Keywords: Redundant Robot Arms, High Precision, Pseudoinverse, Difference Formula, Motion Planning

I. INTRODUCTION

As a result of technological advancements, the mechanical arm has become indispensable in numerous industries and is capable of performing a wide range of jobs, including welding, assembling, handling, maintenance, and painting [1-3]. For different needs, robot arms with different degrees of freedom have been designed successively, such as the UR arm [4] and the KUKA arm [5]. According to the number of degrees of freedom, the robot arms can be divided into redundant and non-redundant robot arms. If the robot arm has more degrees of freedom than is required to perform a given end trajectory tracking task, the robot arm may be considered redundant [1-3].In contrast, redundancy arms have more operating space and more flexibility, making some functional requirements that are specific and non-redundancy difficult to achieve. Due to its unique advantages, the redundancy robot arm is widely used in the industrial, medical, and educational fields.

How to efficiently design the movement of the redundancy robot arm is a key topic in the application study [6-7].For the motion planning of the redundancy manipulator, many research scholars and engineering practitioners have launched different levels of exploration and designed and developed a variety of effective motion planning schemes [1-3,6-10].Among these motion planning schemes, the more classical and widely used are the pseudo-inverse schemes. For example, Lee and Buss proposed an obstacle avoidance planning scheme based on Jacobi transpose [8], Guo et al. proposed a pseudo-inverse type motion planning scheme with noise resistance [9], and Safeea et al. proposed an improved damping least squares method to realize the repeated motion planning [10] of a redundancy robot arm. It is worth pointing out that these schemes are only designed for specific planning purposes (e.g., obstacle avoidance planning, noise-resistant planning, repeated motion planning) and do not have more exploration on the further improvement of the accuracy of motion planning. Based on the existing research basis, this paper proposes a new pseudo-inverse type scheme with high motion planning accuracy and verifies the effectiveness and superiority of the proposed high-precision motion planning scheme through theoretical analysis and simulation.

II. HIGH-PRECISION MOTION PLANNING SCHEME

This part creates a new, highly precise motion planning scheme for the redundancy robot arm that differs from the earlier schemes and theoretically examines its characteristics.

[1,2] ZX-YZ School of Network Science, Haikou University of Economic.Haikou,571127,Hainan,China;
[2] School of Information and Communication Engineering, Hainan University.Haikou,570228,Hainan,China;
[3] Hainan College of Economics and Business.Haikou,570000,Hainan,China;
*Corresponding author: chaichaiyuan@126.com;

A. Foundation of movement planning

In the redundancy robot arm investigation, forward-inverse kinematics is a key component[11]. Positive kinematics is often related to the modeling of mechanical arms; for general redundancy mechanical arms, it can be modeled according to Denavit-Hartenberg parameters and derive the following uniform kinematic equations:

$$f(q(t)) = p(t) \tag{1}$$

Where, $f(\cdot): R^n \to R^m$ represents the nonlinear mapping, $q(t) \in R^n$ represents the joint angle of the robot arm, $p(t) \in R^m$ is the position of the robot arm at the end actuator, and $t \in R$ represents the time. Thus, the positive kinematics of the redundancy robot arm can be described as, given the joint angle $q(t)$, the position $p(t)$ of the end-effector can be determined by the forward calculation of the kinematic equation (1).

Consequently, given the end effector's position, the inverse kinematics of the redundancy robot arm can be described as $p(t)$. Through the reverse calculation of the kinematic equation (1), the joint angle $q(t)$ of the mechanical arm is solved, so as to complete the motion planning of the mechanical arm [1-5,15].

The motion planning of the redundancy robot arm is frequently examined at the velocity layer because of the nonlinearity of the kinematic equations (1). (i.e., avoid the direct solution of the kinematic equations). Guide (1) to obtain the kinematic equation of the following velocity layer:

$$J(q(t))\dot{q}(t) = \dot{p}(t) \tag{2}$$

Where, $J(q(t)) \in R^{m\times n}$ represents the nonlinear mapping, $\dot{q}(t) \in R^n$ represents the joint velocity of the robot arm, $\dot{p}(t) \in R^m$ represents the time derivative of the end position $p(t)$ of the robot arm.For the redundancy robot arm, $n > m$ .Therefor, given $p(t)$and $\dot{p}(t)$, there will be multiple (or even infinite number) $q(t)$ and $\dot{q}(t)$ that can satisfy the kinematic equations (1) and (2).

According to the kinematic equation (2) and considering the feedback of error on the basis of (1), the following pseudo inverse scheme commonly used in the motion planning of redundancy [1-3,6-7,11]:

$$\dot{q}(t) = M(q(t))(\dot{p}(t) - \mu(f(q(t)) - p(t))) + (I - M(q(t))J(q(t)))u(t) \tag{3}$$

Where $M(q(t)) \in R^{n\times m}$ represents the pseudo-inverse matrix of the Jacobi matrix, $\mu \in R$ represents the error feedback coefficient, $I \in R^{n\times m}$ represents the identity matrix,and $u(t) \in R^n$ represents the arbitrary vector determined according to the optimization criterion.

Setting a different $u(t)$ in (3) enables the redundancy robot arm to achieve different purposes, such as obstacle avoidance planning, repeated motion planning, etc. In particular, when $u(t) = 0$, (3) can be further described as

$$\dot{q}(t) = M(q(t))(\dot{p}(t) - \mu(f(q(t)) - p(t))) \tag{4}$$

From a mathematical perspective, the motion planning scheme (4) is an ordinary differential equation, so the "ode15s" instruction in MATLAB can be used to simulate it [13].

B. Description of the protocol

In order to meet the requirements of high precision in practical engineering, on the basis of the motion planning scheme (4), this paper specifically discusses and designs a new scheme with high motion planning accuracy for the redundancy mechanical arm. Since scheme (4) is described in continuous time, it can be discretized by using the difference formula. The Euler difference formula in the existing difference formula is the simplest and most classical [13]. Details are as follows:

$$\dot{q}_k = \dot{q}(t = k\sigma) = \frac{q_{k+1} - q_k}{\sigma} \tag{5}$$

Where, $q_k = q(t = k\sigma)$, $\sigma \in R$ denotes the sampling time, subscript $k = 0,1,2\cdots$. The Euler difference formula (5) is used to discretize the continuous motion planning scheme (4), and then the following discrete motion planning scheme can be obtained.

$$q_{k+1} = q_k + M(q_k)(\sigma\dot{p}_k - h(f(q_k) - p_k)) \tag{6}$$

Where, $\dot{p}_k = \dot{p}(t = k\sigma)$, $p_k = p(t = k\sigma)$, $h = \mu\sigma \in R$ indicates the step length. However, when the protocol (6) is used for the redundancy robot arm, the corresponding motion planning accuracy is not high.

In the same way as Euler difference formula (5), reference documentation [14] constructs the following Taylor difference formula with x cutoff error:

$$\dot{q}_k = \frac{24q_{k+1} - 5q_k - 12q_{k-1} - 6q_{k-2} - 4q_{k-3} + 3q_{k-4}}{48\sigma} \tag{7}$$

Since the Euler difference formula (5) only has a cutoff error of $O(\sigma)$, the Taylor difference formula (7) is better than the Euler difference formula (5). Furthermore, the Taylor difference formula (5) is used to discrete the continuous motion planning scheme (4), and the discrete motion planning scheme can be obtained:

$$q_{k+1} = \frac{5}{24}q_k + \frac{1}{2}q_{k-1} + \frac{1}{4}q_{k-2} + \frac{1}{6}q_{k-3} - \frac{1}{8}q_{k-4} + M(q_k)(2\sigma\dot{p}_k - h(f(q_k) - p_k)) \tag{8}$$

Where step length $h = 2\mu\sigma \in R, k = 4,5,6...$ Discrete scheme (8) is a new scheme for high precision motion planning for redundancy arm proposed in this paper. For scenario (8), its iterative calculation requires values of five joint angles. Therefore, given the initial value q_0 of the redundant mechanical arm joint angle, the iterative calculation of scheme (6) is used to determine the other four numerical values. The details are as follows:

$$\begin{cases} q_1 = q_0 + M(q_0)(\sigma\dot{p}_0 - h(f(q_0) - p_0)) \\ q_2 = q_1 + M(q_1)(\sigma\dot{p}_1 - h(f(q_1) - p_1)) \\ q_3 = q_2 + M(q_2)(\sigma\dot{p}_2 - h(f(q_2) - p_2)) \\ q_4 = q_3 + M(q_3)(\sigma\dot{p}_3 - h(f(q_3) - p_3)) \end{cases} \tag{9}$$

According to the initial calculation of (9) and the iterative calculation of the high-precision motion planning scheme (8), the joint angles of the redundant manipulator at different times during the task cycle can be obtained, that is $\{q_k, k = 0,1,2,...,T/\sigma\}$, where represents the cycle of the trajectory tracking task.

If these joint angles maintain the planning error of the end actuator $e_k = f(q_k) - p_k \in R^m$ within a small numerical range (e. g., 10^{-7} or 10^{-8} order of magnitude), the motion planning of the redundant manipulator is completed.

C. Theoretical analysis

This subsection theoretically analyzes the properties of the proposed high-precision dynamic planning scheme (8).

Lemma 1: The high-precision motion planning scheme (8) proposed in this paper has zero stability and 4 order consistency.

Evidence: High-precision motion planning scheme (8) Characteristic polynomial is as follows:

$$\phi(\vartheta) = \vartheta^5 - \frac{5}{24}\vartheta^4 - \frac{1}{2}\vartheta^3 - \frac{1}{4}\vartheta^2 - \frac{1}{6}\vartheta + \frac{1}{8} \tag{10}$$

Since the five roots of $\phi(\vartheta) = 0$ are in the unit circle, the high precision motion planning scheme (8) has zero stability. On the other hand, the Taylor difference formula (7) has a $O(\sigma^3)$ cutoff error, that is

$$\dot{q}_k = \frac{24q_{k+1} - 5q_k - 12q_{k-1} - 6q_{k-2} - 4q_{k-3} + 3q_{k-4}}{48\sigma} + O(\sigma^3) \tag{11}$$

Using equation (11) to discretize the continuous motion planning scheme (4)

$$q_{k+1} = \frac{5}{24}q_k + \frac{1}{2}q_{k-1} + \frac{1}{4}q_{k-2} + \frac{1}{6}q_{k-3} - \frac{1}{8}q_{k-4} + M(q_k)(2\sigma\dot{p}_k - h(f(q_k) - p_k)) + O(\sigma^4) \tag{12}$$

Omitting $O(\sigma^4)$ in formula (12), we can further obtain

$$q_{k+1} = \frac{5}{24}q_k + \frac{1}{2}q_{k-1} + \frac{1}{4}q_{k-2} + \frac{1}{6}q_{k-3} - \frac{1}{8}q_{k-4} + M(q_k)(2\sigma\dot{p}_k - h(f(q_k) - p_k)) \tag{13}$$

Obviously, solution (12) is the high-precision motion planning solution (8). This shows that the high-precision motion planning scheme (8) has a truncation error of $O(\sigma^4)$. Therefore, it can be determined that the high-precision motion planning scheme (8) has fourth-order consistency.

Lemma 2: The high-precision motion planning scheme proposed here (8) makes the planning error of the redundant robot arm have a change mode of $O(\sigma^4)$.

Proof: Since the high-precision motion planning scheme (8) is zero-stable and consistent, it can be further determined that the scheme is convergent [15] and converges with a truncation error of $O(\sigma^4)$. And, when k is large enough, the following results are obtained:

$$q_k = q_k^* + O(\sigma^4) \tag{14}$$

Where $q_k^* = q^*(t = k\sigma) \in R^n$ represents the theoretical solution of kinematic equation (1), that is, $f(q_k^*) = p_k$. Based on (13) and combined with Taylor expansion principle, we can get it.

$$f(q_k) = f\left(q_k^* + O(\sigma^4)\right) = f(q_k^*) + J(q_k^*)O(\sigma^4) + O(\sigma^8) = f(q_k^*) + J(q_k^*)O(\sigma^4) \tag{15}$$

Based on the expansion of Taylor (14), the following results can be obtained:

$$\| e_k \|_2 = \| f(q_k) - p_k \|_2 = \| J(q_k^*)O(\sigma^4) \|_2 \le \| J(q_k^*) \|_F \| O(\sigma^4) \|_2 \tag{16}$$

Where, $\|\cdot\|_F$ represents the Frobenius norm. If redundancy robot arm motion planning does not appear singular, then $\| J(q_k) \|_F$ is bounded. The $\| e_k \|_2 \le \| O(\sigma^4) \|_2$ is available as per (15). This means that the high-precision motion planning scheme (8) gives the planning error of the end effector of the redundant robot arm a change pattern of $O(\sigma^4)$.

It should be noted that the error change mode of $O(\sigma^4)$ means that the sampling time σ is reduced by 10 times and the corresponding row error is reduced by 10000 times (or, the accuracy is increased by 100000 times). Obviously, according to such a change mode and setting the appropriate sampling time, the scheme (8) proposed in this paper can make the motion planning of the redundancy manipulator with very high precision.

III. Simulation validation

This section simulates the motion planning scheme (6) and (8) based on the plane five-link manipulator and UR manipulator, and verifies the effectiveness and superiority of the proposed high-precision motion planning scheme (8) through comparative simulation results.

A. Flat five-link robot arm

In the simulation of this subsection, the end effector of the flat five-link manipulator is expected to complete the tracking of the tricuspid valve trajectory. The period of the track tracked is 10 seconds and the initial value of the robot arm joint angle is $q_0 = [\pi/18; \pi/18; \pi/18; \pi/18; \pi/18]$ radian. The corresponding simulation results are shown in Figures 1 to Figure 3.

Fig. 1 is the simulation results of the trajectory tracking of the flat five-link robot arm using the motion planning scheme (6) and setting $\sigma = 0.01$ and $h = 0.15$. As can be seen from Fig. 1, the end effector of the robot arm successfully completed the task of trajectory tracking in the plane, with a corresponding maximum planning error of 8.32672×10^{-4} m .These results show the effectiveness of the motion planning scheme (6) and that the Euler difference formula (5) can realize the dispersion treatment of the continuous motion planning scheme (4).

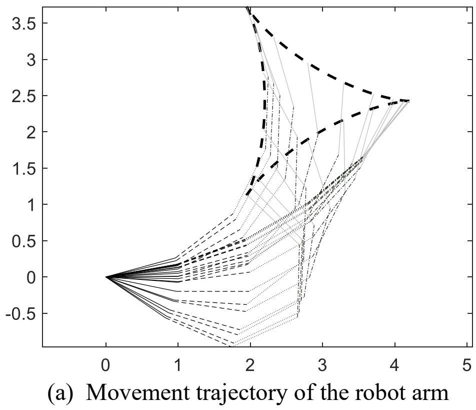

(a) Movement trajectory of the robot arm

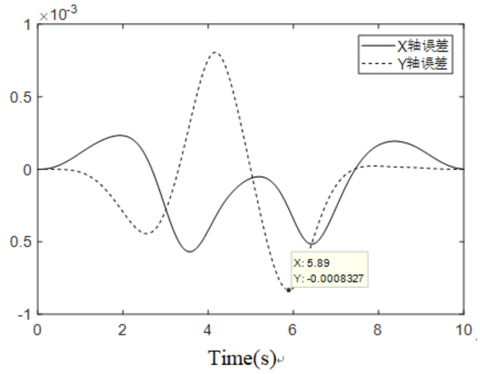

(b) End planning error

Figure 1 The simulation results using the motion planning scheme (6) and setting $\sigma = 0.01$ and $h = 0.15$

Fig. 2 is the simulation result of tracking the tricuspid valve trajectory of the plane five-link manipulator using the high-precision motion planning scheme (8). As can be seen from Fig. 2, the robot arm end actuator also successfully completed the task of trajectory tracking in the plane, with a corresponding maximum planning error of 4.85427×10^{-7} m. These results show the effectiveness of the high-precision motion planning scheme (8) and also show that the Taylor differential formula (7) can effectively realize the discrete treatment of (4). Moreover, it can be seen by comparing Figure 1 (b) and Figure 2 (b) that the maximum planning error obtained by adopting scheme (8) is significantly less than the maximum planning error obtained by scheme (6). From this perspective, the high-precision motion planning scheme (8) is superior to the motion planning scheme (6).

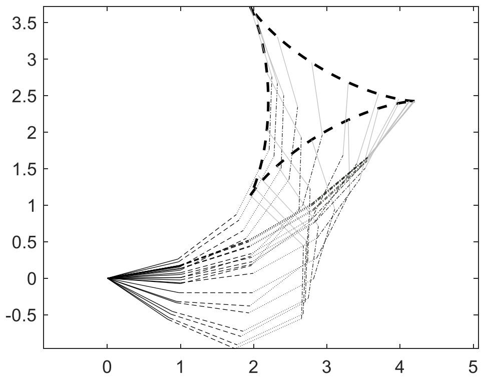

(a) The robot arm movement trajectory

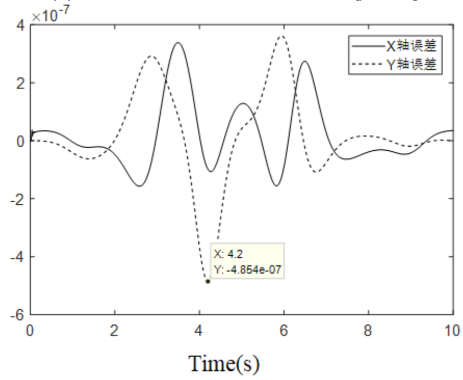

(b) End planning error

Figure 2 shows the simulation results using the motion planning scheme (8) and setting $\sigma = 0.01$ and $h = 0.15$

Further, reduce a from 0.01 to 0.001, the protocol (8). The results in Fig. 3 show that the end effector of the robot arm completes the trajectory tracking task in-plane with a small planning error. Comparing Fig. 2 (b) and Fig.3 (b), σ decreases by 10 times, and the maximum end planning error of the robot arm decreases by 10,000 times, from the order of 10^{-7} to the order of 10^{-11}.

Adopt a high-precision motion planning scheme (8) to reduce the σ. It can significantly improve the track tracking accuracy of the end of the mechanical arm, so as to meet the specific high-precision requirements in the actual engineering, and reflect the necessity of the proposed high-precision motion planning scheme (8).

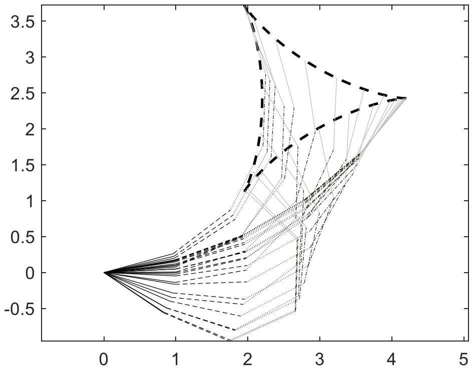

(a) The robot arm movement trajectory

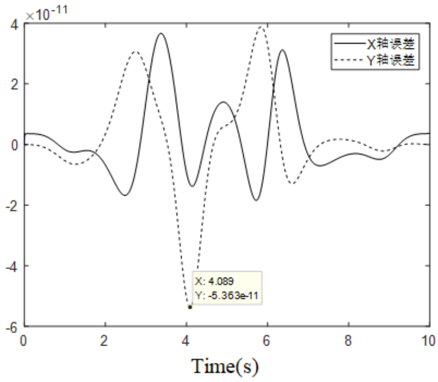

(b) End planning error

Figure 3 shows the simulation results using the motion planning scheme (8) and setting $\sigma = 0.001$ and $h = 0.15$

B. PUMA560 robot arm

In the simulation of this subsection, the end effector of the PUMA560 robot arm expects to complete the tracking of the trajectory. The period of track tracking was 10 seconds, and the initial value of the joint angle of the robot arm was $q_0 = [0;0;0;0;0;0]$ arc. The corresponding simulation results are shown in Figures 4 and Figure 5 and Table 1.

Fig. 4 and Fig. 5 show the simulation results of using the high-precision motion planning scheme (8) and tracking the four-point internal ycloid trajectory by setting $\sigma = 0.01$ and $\sigma = 0.001$ for the PUMA560 manipulator respectively. As can be seen from Fig. 4 and Fig. 5, the end effector of the robot arm successfully performed the task of trajectory tracking in space, with the corresponding maximum end planning error of 1.57055×10^{-7} m and 2.40417×10^{-11} m, respectively. This indicates that the PUMA560 robot arm achieves the purpose of motion planning and thus verifies the effectiveness of the protocol (8). Moreover, the comparison results of Fig. 4 (b) and Fig. 5 (b) again reflect the importance of sampling time σ for the high-precision motion planning scheme (8), i. e., reducing σ can effectively improve the motion planning accuracy of scheme (8) in the redundancy robot arm.

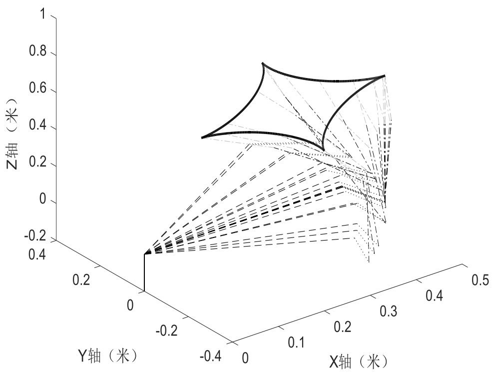

(a) The robot arm movement trajectory

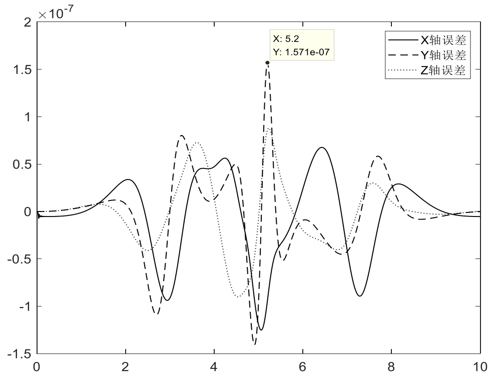

(b) End planning error

Figure 4 Simulation results with a high-precision motion planning scheme (8) and setting $\sigma = 0.01$ and $h = 0.2$

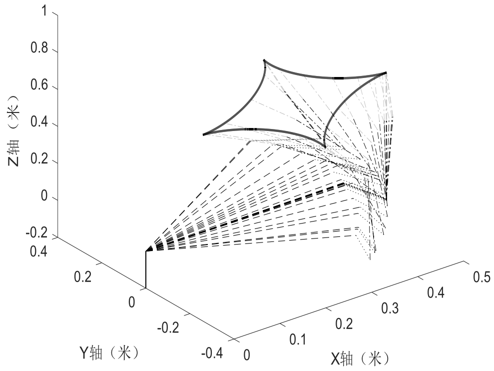

(a) The robot arm movement trajectory

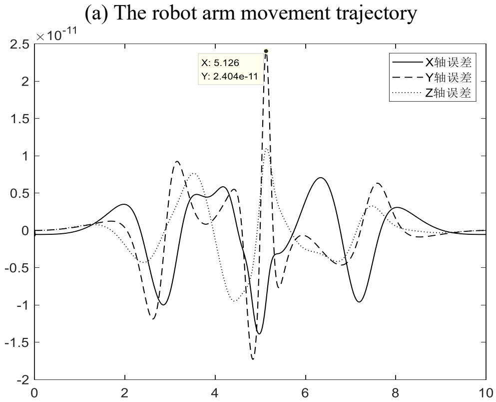

(b) End planning error

Figure 5 The simulation results with high precision motion planning scheme (8) and setting $\sigma = 0.001$ and $h = 0.2$

For further study, changing the value of sampling time σ and step *h*, the high-precision motion planning scheme (8) is used to track the trajectory of the PUMA560 arm; the maximum value of the corresponding end planning error is shown in Table 1. The data in Table 1 again demonstrate the effectiveness of the high-precision motion planning scheme (8). More importantly, combining the results of Fig. 4 and Fig. 5 and Table 1, the following conclusions can be obtained:

a). For the high-precision motion planning scheme (8), when the sampling time is reduced by 10 times, the maximum planning error at the end of the PUMA560 mechanical arm is reduced by 10,000 times. In other words, the planning accuracy increases by 10,000 times. This indicates that the scheme (8) has an error change pattern of $O(\sigma^4)$, which complies with the theoretical results of Lemma 2.

b). The performance of the high-precision motion planning scheme (8) can be further improved by increasing the value of *h*; namely, the motion planning accuracy of the redundancy mechanical arm can be improved with the increase of *h*.

Therefore, setting the sampling time and step length respectively ensures that the scheme (8) can have good performance, which can have high motion planning accuracy when applied to the redundancy mechanical arm. The above simulation results well demonstrate the effectiveness and superiority of the proposed high-precision motion planning scheme (8).

Table 1 sets the maximum end programming error of the manipulator arm at different σ and h

	$\sigma = 0.1$	$\sigma = 0.01$	$\sigma = 0.001$
$h = 0.1$	3.8937×10^{-4}	2.0870×10^{-7}	4.6988×10^{-11}
$h = 0.2$	3.5628×10^{-4}	1.5706×10^{-7}	2.4042×10^{-11}
$h = 0.3$	3.2502×10^{-4}	1.2686×10^{-7}	1.6100×10^{-11}

IV. CONCLUSION

In this paper, the Taylor difference formula (7) is used to discretize the continuous motion planning scheme (4), thus proposing a new scheme with high motion planning accuracy (8) for the redundancy mechanical arm. Then the proposed high-precision motion planning scheme (8) is analyzed from the theoretical level, and it shows that the scheme has the error change pattern of $O(\sigma^4)$. The comparative simulation results of the plane five-link manipulator and the PUMA560 manipulator show the effectiveness and superiority of the high-precision motion planning scheme (8). These results also verify the $O(\sigma^4)$ error variation pattern of scheme (8) when applied to the redundancy robot arm. By appropriately reducing the sampling time σ and increasing the step length h, it can significantly improve the performance of the scheme (8), so as to realize the high-precision motion planning of the redundancy mechanical arm. Finally, it is worth mentioning that the research in this paper can be extended to the discretization of the continuous motion planning scheme (3), so as to derive more new schemes with high precision and different goals (such as obstacle avoidance planning and repeated motion planning, etc.) for the redundancy mechanical arm.

ACKNOWLEDGMENT

Thanks to the Education Department of Hainan Province for the funding of this project, which is supported by the Education Department of Hainan Province,project number:Hnjg2024-129.

REFERENCES

[1] Siciliano B, Sciavicco L, Oriolo G.(2009) robots: modeling, planning and control. Springer-Verlag, London.

[2] Zhang Y, Jin L.(2017). Robot manipulator redundancy resolution.Wiley, Hoboken.

[3] Ceccarelli M.(2022). Fundamentals of Mechanics of robot Manipulation. Second Edition. Springer-Verlag, Switzerland.

[4] Kebria P M, Al-Wais S, Abdi H, Nahavandi S(2016). Kinematic and dynamic modelling of UR5 manipulator. IEEE SMC, pp. 4229-4234.

[5] Sturz Y R, Affolter L M, Smith R S.(2017). Parameter identification of the KUKA LBR iiwa robot including constraints on physical feasibility. IFAC-PapersOnLine. 50(1): 6863-6868.

[6] Tan Min, Wang Shuo. (2013) Research progress in robots. Journal of Automation. 39(07):963-972.

[7] Tang Yongxing, Zhu Zhanxia, Zhang Hongwen, et al. (2023). Overview of robot motion planning methods. Aeronautical Journal, 44 (02): 181-212.

[8] Guo D, Xu F, Yan L.(2018). New pseudoinverse-based path planning scheme with PID characteristic for redundant robot manipulators in the presence of noise . IEEE Trans. Control Syst. Technol. 26(6): 2008-2019.

[9] Safeea M, Bearee R, Neto P.(2021). A modified DLS scheme with controlled cyclic solution for inverse kinematics in redundant robots . IEEE Trans. Ind. Inform, 17(12): 8014-8023.

[10] Leng S, Wu K, Ju H, (2019). Summary of the kinematic modeling and solution methods of the robot arm. Journal of Astronautics, 40 (11): 1262-1273.

[11] Jin L, Li S, Yu J, He J, Robot manipulator control using neural networks: A survey [J]. Neurocomputing, 2021, 285: 23-34.

[12] Guo D, Nie Z, Yan L.(2017).Novel discrete-time Zhang neural network for time-varying matrix inversion. IEEE Trans. Syst., Man, Cybern. 47(8): 2301-2310.

[13] David F G, Desmond J H(2010). Numerical methods for ordinary differential equations: initial value problems. Springer, London.

[14] H. Yang, D. Li, X. Xu and H. Zhang.(2022). An Obstacle Avoidance and Trajectory Tracking Algorithm for Redundant Manipulator End.IEEE Access, vol. 10, pp. 52912-52921.